Available online at www.sciencedirect.com
ScienceDirect
Journal of Catalysis 251 (2007) 271–280
JOURNAL OF CATALYSIS
www.elsevier.com/locate/jcat

Inter-relationship between Pt oxidation states on TiO_2 and the photocatalytic mineralisation of organic matters

Wey Yang Teoh [a], Lutz Mädler [b], Rose Amal [a,*]

[a] *ARC Centre of Excellence for Functional Nanomaterials, School of Chemical Sciences and Engineering, The University of New South Wales, Sydney, NSW 2052, Australia*

[b] *Department of Chemical and Biomolecular Engineering, University of California, Los Angeles, 405 Hilgard Avenue, Los Angeles, CA 90095, USA*

Received 19 June 2007; revised 9 August 2007; accepted 10 August 2007

Available online 19 September 2007

Abstract

The inter-relationship between Pt oxidation state dynamics and the TiO_2 photocatalysis of three groups of organic compounds (carboxylic acid, alcohol and phenolics) was investigated. Repetitive photocatalytic mineralisation of formic acid over the as-prepared Pt(II)/TiO_2 produced free formate radicals which partially reduced Pt(II) to Pt(0, II)/TiO_2. Further repetitive dark mineralisation of formic acid over this pretreated catalyst was as effective as the as-prepared sample under UV-A illumination. As for the photocatalytic mineralisation of methanol, the usually reported current doubling effect which would result in the reduction of Pt was not observed under the studied air-equilibrated condition and low organic concentration. However, the photocatalytic mineralisation of methanol was enhanced over formic acid-pretreated catalyst compared to the as-prepared and phenol-pretreated samples, highlighting the beneficial and detrimental effects of Pt(0) and Pt(IV), respectively. The enhancement was partially attributed to the favourable intimate dark catalytic interaction between Pt(0) and methanol. The photocatalytic mineralisation rates of phenol over as-prepared and formic acid-pretreated catalysts were found to be limited by the benzoquinone/hydroquinone short-circuit equilibrium. The photocatalytic mineralisation of trihydroxybenzene, the immediate product after the short-circuit equilibrium, over as-prepared Pt/TiO_2 was faster relative to phenol and more so over the formic acid-pretreated sample. This corroborates the rate-limiting equilibrium while also demonstrates the beneficial effect of Pt(0). The enhancement effects on these phenolic compounds were in qualitative agreement with the observed dark catalytic mineralisation.

Keywords: Photocatalysis; Dark catalysis; Pt/TiO_2; Flame spray pyrolysis; XPS; Oxidation states; Formic acid; Methanol; Phenolics

1. Introduction

Deposition of Pt is one of the most commonly applied techniques to improve the overall photocatalytic performance of TiO_2. Its presence is encountered in a wide range of photocatalytic reactions such as water splitting [1–5], environmental remediation [6–9] and organic syntheses [10–13], among many others. Compared to other noble metals such as Ag [14–16], Pd [17] and Au [18,19], Pt [7,20–24] is an excellent metal candidate for these reactions because of its large work function. This results in a large Schottky barrier, the electronic potential barrier at the metal–semiconductor heterojunction, at the Pt–TiO_2 contact region and hence allows for efficient photogenerated electrons trapping. At the same time, Pt/TiO_2 is also known for its dark catalytic properties even under ambient aqueous conditions. For instance, Pt deposits are commonly added as co-catalyst for photocatalytic water splitting due to its low hydrogen evolution overpotential. We have recently observed dark mineralisation of aqueous organic compounds such as formic acid, oxalic acid and 1,2,3-trihydroxybenzene over Pt/TiO_2 [9].

In photocatalysis, the role of the oxidation state of Pt deposits is often neglected, with assumption that it mostly exists as Pt metal. Depending on the preparation procedure, Pt may exist as Pt(0), Pt(II) and/or Pt(IV). In fact, the Pt oxidation states may also be subjected to dynamic changes under different reaction conditions as will be shown in this work. Studies on the effect of metal oxidation states on photocatalytic oxida-

* Corresponding author. Fax: +61 2 9385 5966.
E-mail address: r.amal@unsw.edu.au (R. Amal).

0021-9517/$ – see front matter
doi:10.1016/j.jcat.2007.08.008

tion of organic compounds are rare. It was not until recently that Lee and Choi [25] reported the enhanced photocatalytic degradation of dichloroacetate, 4-chlorophenol and chloroform in the order of $Pt(0)/TiO_2 > Pt_{ox}(II, IV)/TiO_2 >$ bare TiO_2 for Pt photodeposited on Degussa P25 TiO_2. However, the degradation of trichloroethylene (TCE) and perchloroethylene (PCE) over Pt_{ox}/TiO_2 was found to be worse than that of bare TiO_2. It was suggested that both chlorinated ethylenes interacted detrimentally with Pt_{ox} to form recombination redox cycles.

Prior to the work, only some scattered information regarding the effect of Pt oxidation states on the photocatalytic effect of TiO_2 could be found. Pichat et al. [20] reported a lower photocatalytic activity of H_2 evolution from the aliphatic alcohols over impregnated Pt(0)/P25 compared to Pt_{ox}/P25. The Pt–O bond was suggested to be beneficial to the hydrogenation and dehydrogenation reaction [20]. In terms of gas-phase photocatalytic degradation of acetaldehyde, Pt(0)/P25 was found to be only slightly (15%) more active than Pt_{ox}/P25 [26]. The photocatalysts were prepared in the same way as by Lee and Choi [25]. In the studies by Pichat et al. [20] and Sano et al. [26], neither the Pt oxidation state dynamics after reaction nor the activity of the used photocatalysts were re-evaluated, which would have otherwise provided insightful information regarding the inter-relationship between Pt oxidation states and photocatalytic degradation of organic compounds.

Perhaps some useful hints could also be gained by inspecting the role of sacrificial holes scavenger on the photoreduction of $PtCl_6^{2-}$ on TiO_2 in a typical preparation of Pt/TiO_2 by photodeposition. In one of the earliest works, Kraeutler and Bard [10] reported formation of Pt(0) during photoreduction of $PtCl_6^{2-}$ in the presence of acetic acid under anoxic condition. However, under a similar condition, Koudelka et al. [27] reported formation of a mixture of Pt_{ox}. Nevertheless, the presence of dissolved O_2 and duration of illumination was not clearly indicated in the study. Under an air-equilibrated condition, Lee and Choi [25] were able to synthesise Pt(0) and Pt_{ox} under methanol-rich (1 M) and methanol-deficient (0.1 M) conditions, respectively. Similar results were obtained by Sano et al. [26] under anoxic condition. Propanol was found to be efficient in reducing $PtCl_6^{2-}$ to Pt(0) under anoxic condition [28].

The present study investigates the effect of repeated photocatalytic mineralisation of non-chlorinated organic substrates at low concentration (10 ppm C), a highly relevant figure in removal of organics where real application of TiO_2 photocatalysis is concerned, on the evolution of Pt oxidation states. Formic acid, methanol and phenol, each representing a different organic group, are used as the model organic compounds. The intermediates of phenol, namely benzoquinone (BQ), hydroquinone (HQ) and trihydroxybenzene (THB) are also examined as complementary to the phenol studies. The Pt oxidation states at different stages of reaction are analysed by X-ray photoelectron spectroscopy (XPS) and related to the photocatalytic degradation mechanism of each organic substrate. At the same time, the influence of different Pt oxidation states in the photocatalytic reactivity of the different organic compounds is also investigated.

Although the significance of Pt oxidation states demonstrated in the present work is only limited to the photocatalytic mineralisation of aqueous phase organic matters, the outcome of this study is in principle directly or indirectly relevant also to other catalysis-related applications such as water splitting [1–5], gas-phase photocatalysis [8,29,30], fuel cell methanol oxidation [31] and hydrogenation reactions [32,33], where interactions of Pt and organic matters are crucial. For instance, in this work we report the different dark catalytic effect of various organic compounds as a function of Pt oxidation states. This in turn interacted favourably with the overall photocatalytic reactions.

2. Experimental

A detailed procedure for the synthesis of Pt/TiO_2 by flame spray pyrolysis (FSP) has been described elsewhere [34]. The flame-made 0.5 at% Pt/TiO_2 which was found to be the optimal photocatalyst [34] is used here as the model photocatalyst. In brief, the liquid precursor was prepared by adding a predetermined amount of platinum acetylacetonate (Aldrich, 97%) to a mixture of titanium isopropoxide (TTIP, Aldrich, purity > 97%)/xylene (Riedel–de Haen, 96%)/acetonitrile (Fluka, 99.5%) in the volume ratio of 20/55/25. The mixture was delivered to the nozzle tip (1.5 bar) at 5 mL/min where it was dispersed by 5 L/min of O_2. The dispersed droplets were ignited by a surrounding O_2/CH_4 (3.2/1.5 L/min) flame forming a main core flame spray. Additional 5 L/min of sheath O_2 was issued through the outer most ring of the spray burner.

The photocatalytic studies were conducted in a 200 mL closed-system slurry-type spiral reactor as described by Abdullah et al. [35] and also in our earlier work [34,36]. A photocatalyst suspension of 1 g/L adjusted to pH 3.5 ± 0.25 using perchloric acid (Unilab, 99%) was used in all experiments. An impurity carbon burn-off step was carried out by illuminating the slurry with a UV-A lamp (NEC T10 blacklight blue, 20 W) at ambient condition until no further CO_2 could be detected. The slurry was then air-equilibrated before the injection of organic compounds. We will refer the catalyst to "as-prepared" after this treatment. Formic acid (Aldrich, 99%), methanol (Mallinckrodt Chemicals, LC grade), phenol (BDH, 99%), benzoquinone (BQ, Aldrich, 98%), hydroquinone (HQ, Aldrich, ⩾99%), 1,2,3-trihydroxybenzene (THB, Riedel–de Haen, extra pure) and sucrose (Fisons, analytical grade) were used as the model organic compounds. Except for formic acid and THB which undergo rapid dark catalytic mineralisation in the presence of Pt/TiO_2, all other organic compounds were allowed 20 min of dark adsorption. Photocatalytic reaction was initiated by illuminating the suspension with the UV-A lamp. Evolution of CO_2 during the catalytic mineralisation of organic compounds was monitored online based on conductivity measurements (Jenway 4330). For the zeta-potential dynamic studies, similar photocatalytic reaction procedure was carried out in a 0.1 g/L Pt/TiO_2 suspension. A small amount of suspension was withdrawn from the reactor during the reaction at different time. Zeta potential of the particles was measured directly

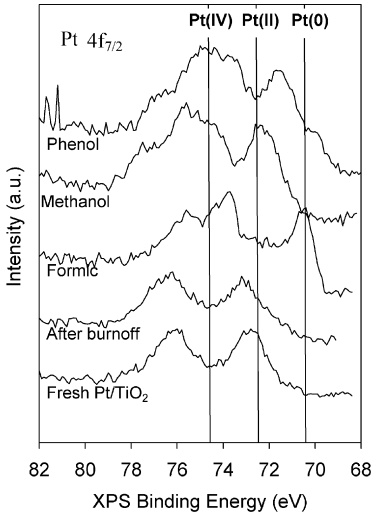

Fig. 1. XPS spectra of freshly prepared FSP Pt/TiO_2, after carbon burn-off and after 10 repeated photocatalytic mineralisation runs of formic acid, methanol and phenol.

by means of electrophoretic mobility on a Brookhaven ZetaPals system.

The Pt oxidation states of fresh and used photocatalysts were analysed using X-ray photoelectron spectroscopy (XPS) on ESCALab220i-XL (VG Scientific). After complete reaction, the photocatalyst was recovered by vacuum filtration (Sartorius) followed by air drying in an oven at 60 °C. Monochromated Al$K\alpha$ was used as the radiation source. Analysis was carried out in a vacuum chamber ($<2 \times 10^{-9}$ mbar). The binding energies of all peaks were referenced to the C 1s line (285.0 eV) originating from surface organic impurities and checked against the binding energy of Ti 2p (458.8 eV) from TiO_2. Peak fittings and deconvolution were performed using the Eclipse (VG Scientific software). Other physicochemical characterisations such as transmission electron microscopy, specific surface area, X-ray diffraction (anatase–rutile composition and crystallite sizes) and CO-pulse chemisorption (Pt dispersion and size) of the as-prepared Pt/TiO_2 have been described in our earlier publication [34].

3. Results and discussion

3.1. Impurity carbon burn-off

All Pt/TiO_2 suspensions were subjected to impurity carbon burn-off by UV-A illumination prior further evaluations. During the burn-off, adsorbed organic impurities on the photocatalyst surface were oxidised to CO_2. This procedure ensures that the origin of CO_2 evolution during mineralisation studies of selected organic compounds at subsequent stages did not originate from pre-adsorbed impurities.

Surface XPS analysis of the fresh FSP-made Pt/TiO_2 revealed pre-dominant amount of Pt(II) (97%) and small quantities of Pt(0) (3%) (Figs. 1 and 2). This is in agreement with similarly prepared Pt/SnO_2 by FSP [37]. However after the carbon burn-off stage, a slight increase in Pt(0) (8%)

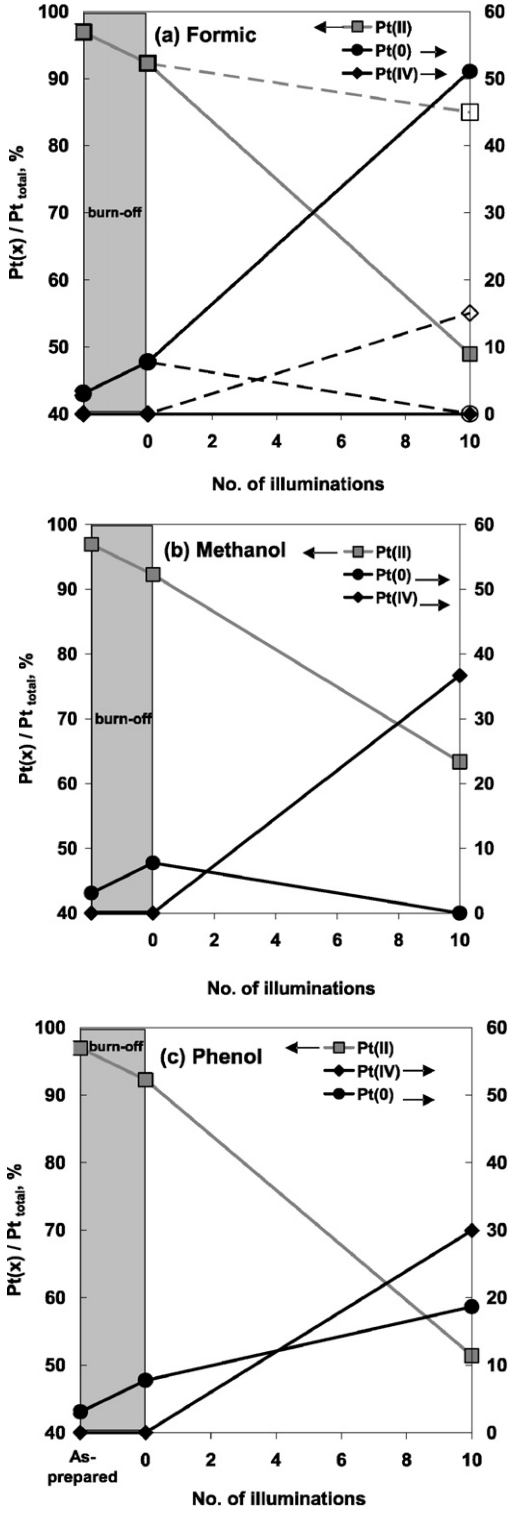

Fig. 2. The Pt oxidation state dynamics during impurity carbon burn-off (grey box) and repetitive photocatalytic mineralisation of 10 ppm C as (a) formic acid, (b) methanol and (c) phenol. The open symbols and broken lines in (a) represent the dark mineralisation of formic acid. Pt(x) is the Pt oxidation state, where $x = 0$, II and IV. Lines drawn are only to illustrate connecting of data points for reference purposes.

content at the expense of the dominant Pt(II) is evident from Figs. 1 and 2. No detectable amount of Pt(IV) was measured from these samples. For convenience, the Pt/TiO_2 pho-

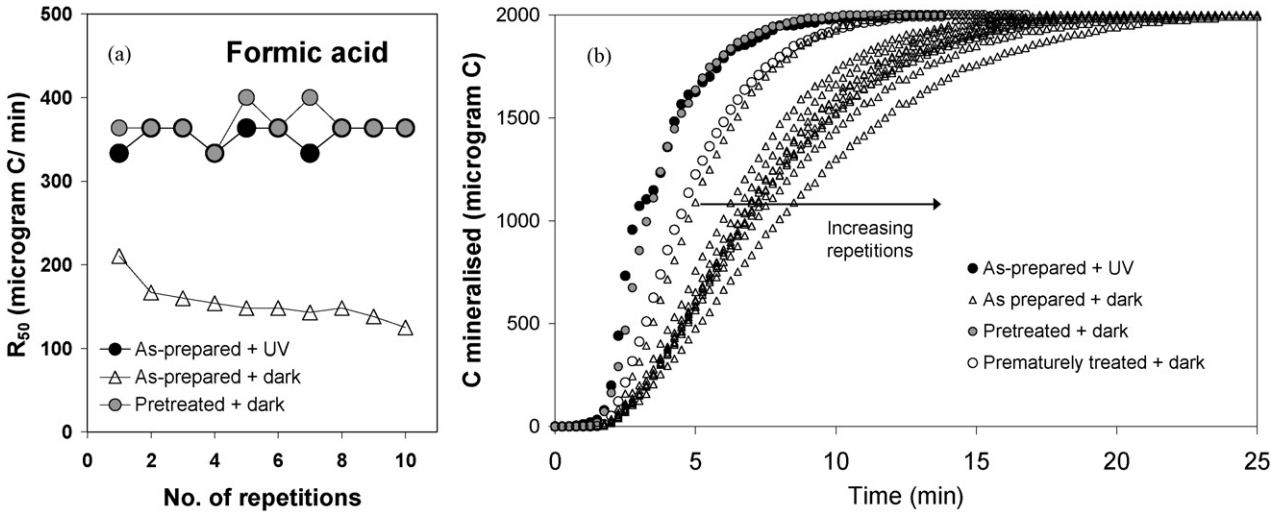

Fig. 3. Repetitive mineralisation of formic acid over as-prepared Pt/TiO_2 under UV illuminations and under dark conditions as well as for formic acid-pretreated Pt/TiO_2 under dark conditions. The data is presented in (a) half-life mineralisation rates (R_{50}) and (b) the corresponding kinetics of mineralisation.

tocatalyst after carbon burn-off is referred to as "as-prepared" Pt/TiO_2.

3.2. Formic acid mineralisation

Figs. 3a and 3b show that dark mineralisation of formic acid (10 ppm C) took place over as-prepared Pt/TiO_2 (open triangles). The mineralisation rates were however much slower than that carried out under UV-A illumination (black circles). In addition, a gradual deactivation was observed over as-prepared catalysts with repetitive dark mineralisation (Figs. 3a and 3b). After 10 repeated dark mineralisation runs, the XPS analysis on the Pt oxidation states showed about 15% of the total Pt being converted to Pt(IV) at the expense of the initially dominant Pt(II) and minor Pt(0) (Fig. 2a, dashed line).

In a separate work, He et al. [38] reported dark oxidation of formic acid over photodeposited Pt on pre-calcined (400 °C, 2 h) TiO_2 (P25)/ITO (indium-tin-oxide) films under aerated condition, also at a much slower rate than under UV illumination. Notably, the procedure of coating photodeposited Pt/TiO_2 (P25) particles onto ITO substrate followed by calcination at the same condition did not yield any formic acid dark oxidation. Although no explanation was given by the authors, it was presumed that the post-calcination of Pt deposits in the latter procedure converted a significant amount of Pt(0) to Pt(IV), a process which could take place even by heating at 150 °C for 15 min in air [39]. The observation by He et al. [38] is consistent with our results that Pt(IV) is detrimental towards formic acid dark mineralisation. The group also reported enhanced formic acid oxidation on continuous O_2 sparging. It is noteworthy in the present work that the deficiency of dissolved O_2 leading to gradual deactivation is ruled out since the Pt/TiO_2 suspension is air-equilibrated equally in each reaction run. The total organic carbon (TOC) analysis of the filtrate at the end of 10 repeated dark mineralisation runs did not detect any significant amount of accumulated, dissolved and non-adsorbed organic matters. Similarly, no presence of adsorbed organic compounds was detected by zeta-potential measurements after each run (not shown). Hence, it can be confirmed that the catalyst deactivation was not due to poisoning by recalcitrant intermediate compounds. Although the exact reaction mechanism remains unclear at this point, it can be readily deduced that formic acid dark mineralisation is a function of Pt oxidation states, with Pt(IV) presenting a detrimental effect.

To further investigate the role of Pt oxidation states, the as-prepared Pt/TiO_2 was subjected to 10-run repetitive photocatalytic mineralisation of formic acid prior to dark mineralisation. Such repetitive mineralisation of formic acid under UV-A illumination increased the Pt(0) content, yielding approximately equal amount of Pt(0) (51%) and Pt(II) (49%) after 10 repetitions (Fig. 2a, solid line). The exact reaction mechanism will be discussed in detail in the subsequent paragraphs. The increase in Pt(0) content and the absence of Pt(IV) did not only prevent the deactivation of Pt catalyst that was observed earlier, but was found to dark mineralise formic acid as efficiently as that under UV-A illumination (Figs. 3a and 3b, grey circles). This is in agreement with our recent studies [9], where photodeposited Pt on Degussa P25 (yielding mainly Pt(0)) at the same metal loading could dark mineralise formic acid as fast as under UV-A illumination. Interestingly, despite the co-existence of Pt(0) and Pt(II) in this work, similar dark and photocatalytic mineralisation rates were observed. Hence it can be concluded from the findings that the dark catalytic mineralisation of formic acid over Pt/TiO_2 increases in the order of Pt(0) > Pt(II) > Pt(IV).

Fig. 3a (black circles) shows constant photocatalytic mineralisation rates ($R_{50} = \sim 360\ \mu g\,C/min$) of formic acid (10 ppm C) over as-prepared Pt/TiO_2 throughout 10 repeated runs under UV-A illumination. This holds despite the evolving Pt oxidation states (Fig. 2a) at every repetition, indicating an independent relationship between the photocatalytic mineralisation rates and Pt oxidation states at the studied conditions. Furthermore, the catalysts pretreated with formic acid under UV-A illumination over 2 repeated runs (10 ppm C each) (defined as "prematurely treated") showed a significant lower dark mineralisation rate ($R_{50} = 222\ \mu g\,C/min$, Fig. 3b, open circles) compared to that

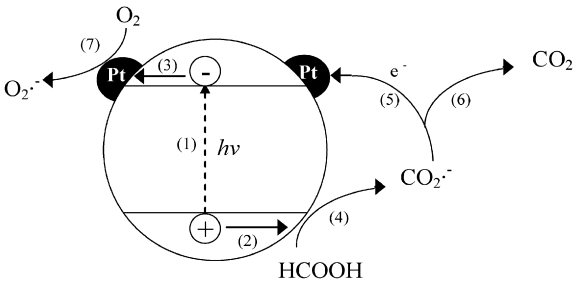

Scheme 1. Proposed mechanism of photocatalytic degradation of formic acid over Pt/TiO_2 in the presence of dissolved O_2. (1) Photogeneration of charge carriers (e^-, h^+) under UV illumination, (2) trapping of h^+ at photocatalyst surface, (3) trapping of e^- at Pt deposits, (4) oxidation of formic acid to formate radical, (5) reduction of Pt deposits by formate radical, (6) mineralisation of formate radical, (7) scavenging of e^- by dissolved O_2. For simplicity, the formation of OH· through photocatalytic oxidation of water or surface titanol species is not shown but is represented by step (2).

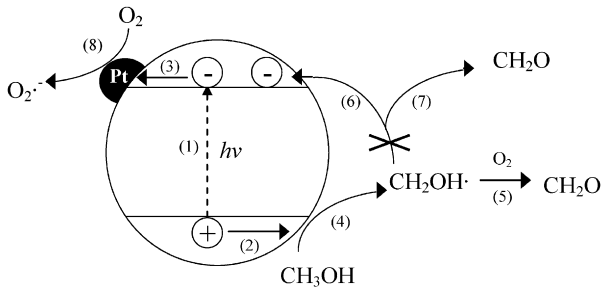

Scheme 2. Proposed mechanism of photocatalytic degradation of methanol over Pt/TiO_2 in the presence of dissolved O_2. (1) Photogeneration of charge carriers (e^-, h^+) under UV illumination, (2) trapping of h^+ at photocatalyst surface, (3) trapping of e^- at Pt deposits, (4) oxidation of methanol to α-hydroxymethyl radicals, (5) oxidation of α-hydroxymethyl radicals to formate radical by dissolved O_2, (6 and 7) the inhibited path of e^- injection of methyl radicals to TiO_2 conduction band to form formaldehyde (current doubling), (8) scavenging of e^- by dissolved O_2. For simplicity, the formation of OH· through photocatalytic oxidation of water or surface titanol species is not shown but is represented by step (2).

carried out under UV-A illumination. This confirms the dominant photocatalytic effect and rules out the possibility of high reaction rates during repeated formic acid photocatalytic mineralisation originating solely from the catalytic effect (at least during the first few repetitions). As expected, only minor dark mineralisation rate enhancement was observed for the prematurely formic acid-treated Pt/TiO_2 compared to the as-prepared sample ($R_{50} = 211\ \mu g\,C/min$).

The origin of Pt(0) as a result of formic acid mineralisation under UV-A illumination could be traced to the (1) Schottky-type trapping of conduction band electrons and (2) reduction by formate radical anion intermediate, $CO_2^-\cdot$ ($E^\circ(CO_2^-\cdot/CO_2) = -1.9\ V_{SHE}$) [41,42]. In the latter case, the photocatalytic oxidation of formate ions by photogenerated holes (or hydroxyl radicals, OH·) is known to generate the highly reductive formate free radicals (Scheme 1). In fact the reductive power of such radical has been demonstrated by Rajeshwar and co-workers [43] to reduce highly electropositive metal ions (Zn^{2+}/Zn^0 ($-0.762\ V_{SHE}$); Cd^{2+}/Cd^0 ($-0.403\ V_{SHE}$); Mn^{2+}/Mn^0 ($-1.185\ V_{SHE}$)) in TiO_2 suspensions. It is noteworthy that the reduction potentials of these metal ions with respect to their respective zero-valent states all lie in between that of TiO_2 conduction band electrons ($E^\circ = -0.4\ V_{SHE}$) [44] and formate radicals. In this work, the effective in situ reduction of Pt deposits through the formation of formate radicals has conveniently allowed the studies of Pt oxidation state effects on photocatalytic oxidation of other organic compounds as described in the following sections. Moreover the complete photocatalytic mineralisation of formic acid and the absence of inorganic elements (such as Cl^-) as side products circumvent investigations of foreign ions interactions during subsequent reaction studies.

3.3. Methanol mineralisation

Repeated photocatalytic mineralisation of methanol at low concentration (10 ppm carbon) resulted in the enhanced formation of Pt(IV) rather than Pt(0) (Fig. 2b). This contradicts to what would be expected from the Schottky-type electrons trapping mechanism and may even appear contradicting the current doubling effect that was postulated by others [45–48]. It is well established that oxidation of methanol by photogenerated holes or OH· in anoxic aqueous forms reducing α-hydroxymethyl radicals, $CH_2OH\cdot$ ($E^\circ(CH_2OH\cdot/CH_2O) = -0.95\ V_{SHE}$) [49]. Under anoxic condition, these radicals could contribute additional electrons to the TiO_2 conduction band (current doubling effect) to form formaldehyde, CH_2O [50]. Although $CH_2OH\cdot$ has a lower reduction potential than $CO_2^-\cdot$, it is energetically possible to reduce Pt(II) to Pt(0) ($E^\circ(Pt^{2+}/Pt^0) = 1.18\ V_{SHE}$). Ohtani et al. [51], for instance, reported reduction of Pt(IV) to Pt(0) during the degradation of ethanol and 2-propanol under argon-saturated condition. However, under the present ambient air-equilibrated conditions, dissolved O_2 molecules could oxidise $CH_2OH\cdot$ directly to formaldehyde and therefore prevent the current doubling effect [52,53] (Scheme 2).

The present experiment was not carried out under anoxic condition as complete mineralisation may not be achieved under such condition [51]. Interestingly, Lee and Choi [25] managed to photodeposit Pt(0) onto P25 TiO_2 from H_2PtCl_6 ($E^\circ(PtCl_6^{2-}/Pt^0) = 0.68\ V_{SHE}$) under air-equilibrated but high methanol concentration (1 M). However, in the same publication, only Pt_{ox} was formed in the low methanol concentration (0.1 M) system even after 120 min of UV illumination. Although no explanation was provided by the authors, it is envisaged that the resultant small amount of generated electrons from current doubling effect (as a result of low methanol concentration) was insufficient to fully reduce $PtCl_6^{2-}$ to Pt(0). The competition between dissolved O_2 and the relatively small amount of $CH_2OH\cdot$ further decreases the net amount electrons available for Pt reduction. The same analogy could be applied to explain the absence of Pt(0) observed in the present work despite repetitive photocatalytic mineralisation of methanol at low concentration (Fig. 2b). The formation of Pt(IV) could be explained by the lack of adsorption of methanol and its intermediates on the photocatalyst surface, as evident from the adsorption dynamic studies (Fig. 4) [36,40], resulting in hole scavenging by the Pt(II) species.

Formic acid-pretreated Pt/TiO_2 (Fig. 5a, black diamonds) exhibited significantly higher rates of methanol mineralisation compared to the as-prepared photocatalyst (open squares). The catalyst was treated in a similar way to that of repetitive photocatalytic mineralisation of formic acid as discussed earlier and therefore has a higher Pt(0) content than that of the as-prepared sample (Fig. 2a). The much faster mineralisation observed for the pretreated photocatalyst indicates strong dependencies of methanol mineralisation on Pt oxidation states, with Pt(0) favouring faster mineralisation. To probe the origin of enhanced methanol mineralisation rates, dark catalytic mineralisation was carried out over the Pt/TiO_2 samples. It is evident from Fig. 5b that significant methanol dark mineralisation rates took place over formic acid-pretreated Pt/TiO_2 in the dark compared to the as-prepared sample. Even though the dark catalytic reaction was slow compared to UV-A illumination, the more pronounced catalytic effect of pretreated Pt/TiO_2 arising from enhanced Pt(0) content is believed to have resulted in favourable interactions during photocatalytic reaction. This is in agreement with the beneficial effect of Pt(0) in catalytic alcohol oxidation, where Pt_{ox} catalyst was known to be detrimental [54]. In a separate study, photodeposited Pt on similarly made bare TiO_2 (as that of FSP-made Pt/TiO_2 in present work) which consisted of mainly Pt(0) also found comparable dark catalytic activity as that of formic acid-pretreated Pt/TiO_2. In both cases, the accuracy of CO_2 evolution detected was in excellent agreement with our total organic carbon (TOC) filtrate analyses. This again provides evidence that the formic acid-pretreated Pt/TiO_2 is sufficient to impose similar dark catalytic activity as the photodeposited samples despite only being partially reduced. The dark methanol mineralisation reported here has also been recently observed by Hu et al. [55] who reported spontaneous gas-phase combustion of methanol/air and ethanol/air gas mixtures over Pt (50–700 nm) immobilised on quartz wool.

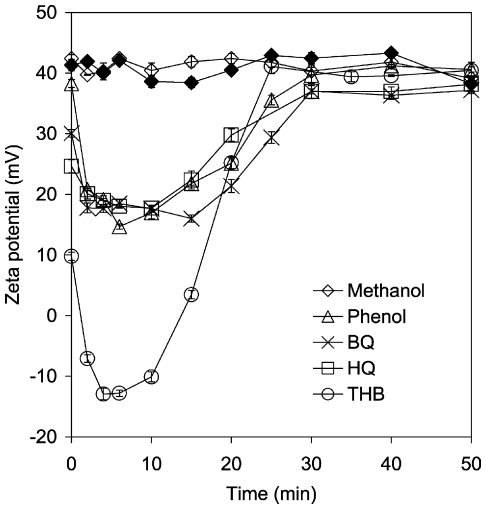

Fig. 4. Zeta-potential dynamics of as-prepared (open symbols) and formic acid-pretreated (solid symbols) Pt/TiO_2 during photocatalytic mineralisation of methanol, phenol, benzoquinone (BQ), hydroquinone (HQ) and trihydroxybenzene (THB).

Fig. 6 shows minimal change in Pt oxidation states of the formic acid-treated photocatalyst after repetitive methanol mineralisation. The result is rather unexpected considering the absence of Pt(IV) increase at the expense of Pt(II) as would be expected from the photocatalytic mineralisation of methanol over as-prepared Pt/TiO_2 (Fig. 2b). As shown in Fig. 4, the adsorption dynamics studies of methanol and its intermediates during photocatalytic reaction as measured by zeta-potential measurements [40,56] did not show significant changes on both as-prepared and formic acid-treated catalysts, thus pointing to the insignificant organic adsorption over a period of 50 min. Hence the adsorption properties of methanol and its intermediate are not a contributing factor to explain the Pt oxidation state dynamics on both as-prepared and formic acid-pretreated catalysts. Although the exact mechanism could not be elucidated at this point, the minimal change in Pt oxidation states on formic acid-pretreated catalysts does however explain the con-

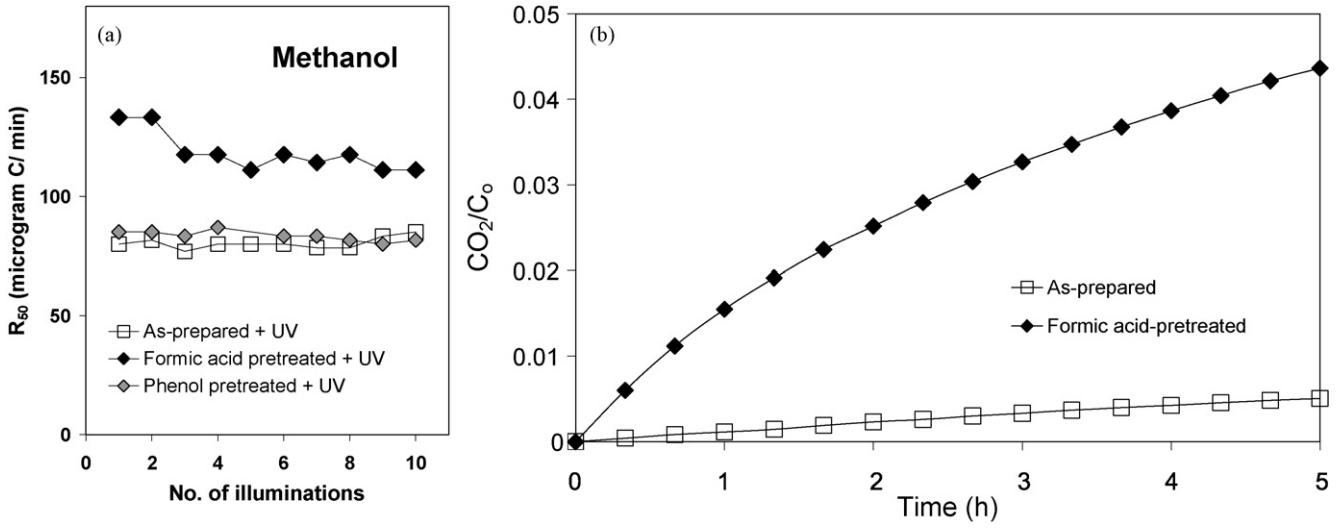

Fig. 5. (a) Repetitive half-life photocatalytic mineralisation rates (R_{50}) of methanol over as-prepared, formic acid- and phenol-pretreated Pt/TiO_2 under UV illuminations and (b) the corresponding dark catalytic mineralisation of methanol as a function of time.

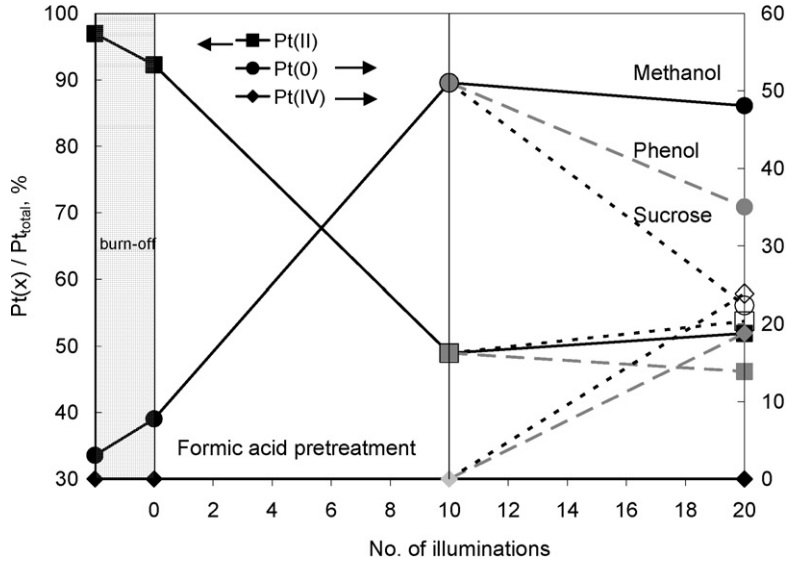

Fig. 6. The Pt oxidation state dynamics during impurity carbon burn-off (grey box) and photocatalytic pre-treatment with formic acid followed by repetitive photocatalytic mineralisation of methanol (black symbols, —), phenol (grey symbols, – –) and sucrose (open symbols, - - -). Lines drawn are only to illustrate connecting of data points for reference purposes.

stant photocatalytic mineralisation rates throughout the course of repetitions (Fig. 5a).

In a further study, the as-prepared Pt/TiO_2 was subjected to pretreatment with phenol instead of formic acid. This increased both Pt(0) content and Pt(IV) content at the expense of Pt(II) (Fig. 2c), as will be discussed in the next section. As evident from Fig. 5a (grey diamonds), similar photocatalytic mineralisation rates as that of as-prepared Pt/TiO_2 were measured. Hence, it can be deduced from such comparisons that the detrimental effect of Pt(IV) overwhelms the effect of Pt(0) for photocatalytic mineralisation of methanol, consistent with our earlier explanation on the role of Pt(IV) during dark catalytic reaction of formic acid.

3.4. Phenol mineralisation

The photocatalytic degradation mechanism of phenol, like formic acid and methanol, is well established and has been extensively studied [57–60]. In most cases, catechol, hydroquinone (HQ), benzoquinone (BQ) and trihydoxybenzene (THB) were identified as intermediate compounds. Fig. 2c shows that repetitive photocatalytic mineralisation of phenol resulted in the co-formation of Pt(0) (19%) and Pt(IV) (30%) species at the expense of Pt(II) (51%). Unlike formic acid, no reductive radical is known to be formed from the photocatalytic degradation of phenol over Pt/TiO_2 [60]. Therefore, Pt(0) can be reasonably ascribed to the Schottky-type accumulation of photogenerated electrons on Pt deposits while Pt(IV) is most likely a result of high extent of organic compound-driven reductive pathway. Photodegradation of phenol has been shown to go through the so-called electron shuttle mechanism in which HQ and BQ exist in a "short-circuiting" equilibrium [57,58,61]. Under UV illumination, HQ can be oxidised by photogenerated holes, OH• or dissolved O_2 to form BQ. BQ in turn can be reduced back to HQ ($E°(C_6H_4O_2/C_6H_6O_2) = 0.6992\ V_{SHE}$)

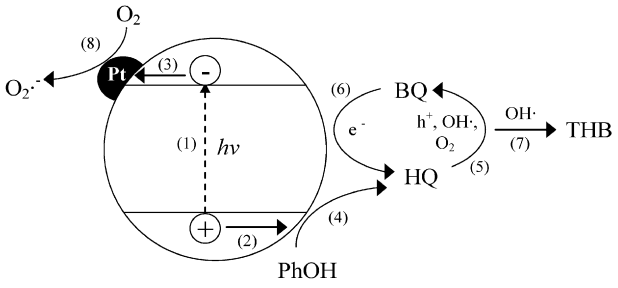

Scheme 3. Proposed mechanism of photocatalytic degradation of phenol over Pt/TiO_2 in the presence of dissolved O_2. (1) Photogeneration of charge carriers (e^-, h^+) under UV illumination, (2) trapping of h^+ at photocatalyst surface, (3) trapping of e^- at Pt deposits, (4) oxidation of phenol (PhOH) to hydroquinone (HQ), (5) oxidation of hydroquinone to benzoquinone (BQ) by h^+, OH• or O_2, (6) reduction of BQ to HQ by e^- (steps 5 and 6 form short-circuiting equilibrium), (7) formation of trihydroxybenzene (THB), the immediate species after the short-circuiting equilibrium species, (8) scavenging of e^- by dissolved O_2. For simplicity, the formation of OH• through photocatalytic oxidation of water or surface titanol species is not shown but is represented by step (2).

through electron scavenging (Scheme 3). In the presence of Pt species, the electrons for the reduction reaction would most likely originate from the accumulated electrons on the Pt deposits, thereby oxidising Pt(0)/Pt(II) to Pt(IV). More importantly, BQ was found to be a very efficient electron scavenger, even outperforming dissolved O_2 for photogenerated electrons on illuminated TiO_2 and ZnO surfaces [62]. It can be seen from this work (Fig. 7a) that, despite the varying Pt oxidation states during repetitive mineralisation of phenol (open triangles), no significant difference with respect to mineralisation rates was observed over the 10 repetitions (Fig. 7a, open triangles).

Unlike formic acid and methanol, pretreatment with formic acid did not have any influence on the overall photocatalytic mineralisation rates (black triangles). No difference in mineralisation rates was observed for the pretreated catalysts throughout

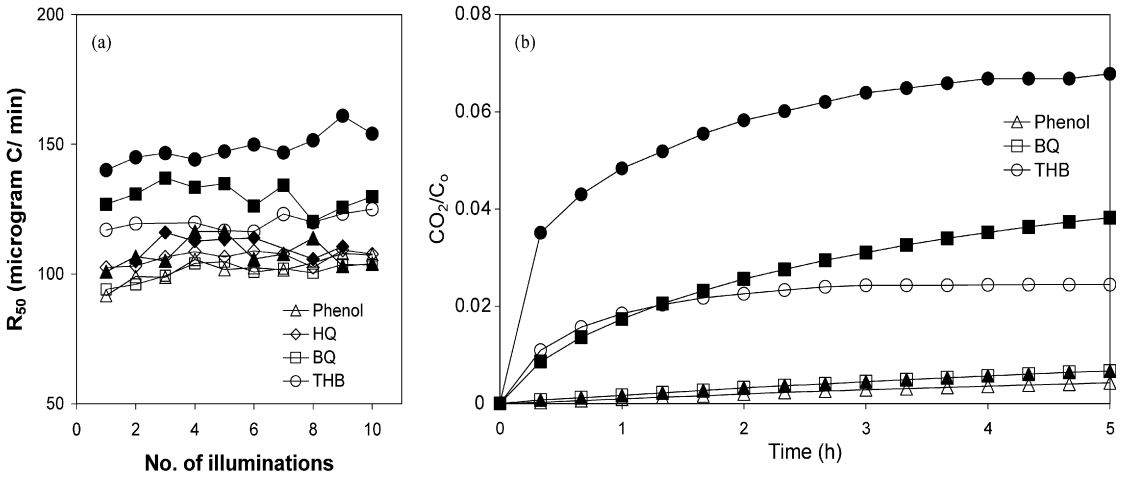

Fig. 7. (a) Repetitive half-life photocatalytic mineralisation rates (R_{50}) of phenol, benzoquinone (BQ), hydroquinone (HQ) and trihydroxybenzene (THB) over as-prepared (open symbols) and formic acid-pretreated (solid symbols) Pt/TiO_2 under UV illuminations and (b) the corresponding dark catalytic mineralisation of phenol, BQ and THB as a function of time.

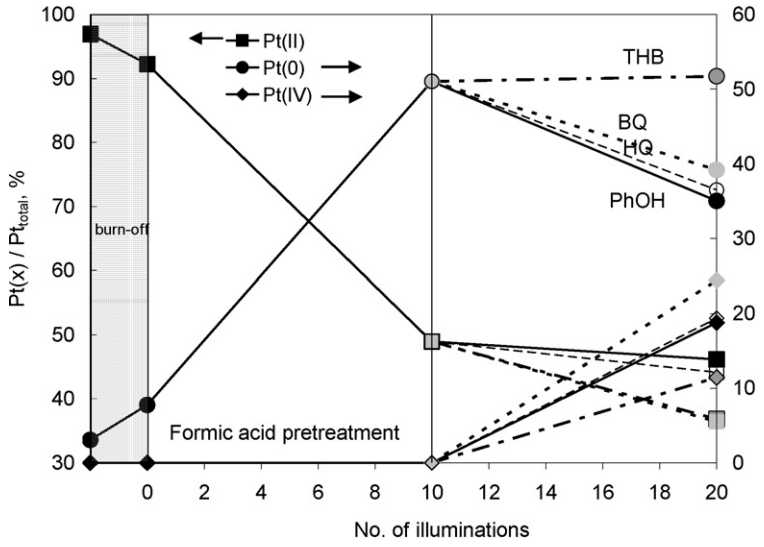

Fig. 8. The Pt oxidation state dynamics during impurity carbon burn-off (grey box) and photocatalytic pre-treatment with formic acid followed by repetitive photocatalytic mineralisation of phenol (black symbols, —), BQ (benzoquinone, light grey symbols, - - -), HQ (hydroquinone, open symbols, – –) and THB (trihydroxybenzene, dark grey symbols, - – -). Lines drawn are only to illustrate connecting of data points for reference purposes.

the 10 repetitions. In both the cases of as-prepared and formic acid-pretreated Pt/TiO_2, little and almost insignificant dark CO_2 evolution was detected (Fig. 7b, triangles), as was also verified by our TOC filtrate analysis. XPS analysis on the formic acid-treated photocatalyst after subsequent repeated mineralisation of phenol showed a decreased Pt(0) and increased Pt(IV) content (Fig. 8), again supporting the postulation of electron shuttle mechanism where conversion of BQ to HQ resulted in the loss of electrons accumulation on Pt deposits.

In order to closely probe the photocatalytic mineralisation of phenol, analogous sets of experiments were carried out on BQ and HQ, the two short-circuiting equilibrium species, and also THB, the immediate species after the equilibrium. Catechol was not chosen as the studied compound since it presents only in a small quantity during photocatalytic degradation of phenol over platinised TiO_2 [60], inferring a less influential species compared to BQ and HQ. Fig. 7a shows comparable photocatalytic mineralisation rates of phenol, BQ and HQ over as-prepared Pt/TiO_2, while a slightly faster mineralisation was observed for THB. The observation confirms the rate-limiting step of BQ/HQ short-circuit equilibrium. To assist the electron shuttle mechanism, it is required the organic substrate to be in intimate contact with the photocatalyst surface through adsorption. Phenol tends to adsorb sparingly on the photocatalyst surface. However upon attacks by OH• and holes, its generated intermediates could adsorb strongly as indicated by the sharp decrease in zeta-potential value as the reaction proceeds (Fig. 4). The significantly lower initial zeta-potential values of Pt/TiO_2 in the presence of BQ (30.06 ± 0.61 mV), HQ (24.64 ± 1.07 mV) and THB (9.79 ± 0.67 mV) compared to phenol (38.26 ± 0.65 mV) further support this observation (Fig. 4). As photocatalytic reaction proceeds, further decrease in zeta potential was observed

due to the strong adsorption of negatively charged carboxylic acid intermediates [36,40,56]. As a result of the low concentration of organic compounds, the change in suspension pH (±0.05) throughout the course of photocatalytic reaction was too minimal to have significant influence on the zeta-potential values. While phenol and all the intermediates studied (BQ, HQ and THB) have similar zeta-potential dynamic profile, the zeta-potential magnitude of THB during photocatalytic reaction is inherently more negative. This is likely to be a result of rapid decomposition of THB giving rise to an instantaneous large quantity of carboxylic acids. Phenol, BQ and HQ had to go through the rate-limiting short-circuit equilibrium step during their photocatalytic mineralisation, which in turn limited the instantaneous amount of THB and hence carboxylic acids produced. The particle zeta potential at the end of mineralisation for all compounds tested converges to approximately +38 mV, corresponding to clean surface free of adsorbed organic impurities.

Like phenol, catalyst pretreatment with formic acid had little effect on the overall photocatalytic mineralisation of HQ (Fig. 7a). However, the mineralisation rates of BQ over pretreated Pt/TiO_2 were significantly higher and more so for THB (Fig. 7a). The fast dark mineralisation rates of BQ and THB over the pretreated Pt/TiO_2 (Fig. 7b) implied an intimate catalytic interaction between the organic compounds and reduced Pt. This in turn contributed to the enhanced photocatalytic mineralisation of BQ and THB. Relating these results to the phenol mineralisation, even though mineralisation of BQ was enhanced over pretreated catalysts, the rate-limiting step and co-existent nature of BQ/HQ prevented a similar degree of improvement. In fact, the rate-limiting short-circuit equilibrium could also explain the mild 24% enhancement in phenol mineralisation observed over Pt/TiO_2 in this work, compared to the similarly made bare TiO_2 [36]. Other reported work on the photocatalytic oxidation of phenol over Pt/TiO_2 prepared by various methods, also found minimal enhancement in terms of overall mineralisation [9,59,60].

As a result of the dominant electron shuttle mechanism, a comparable trend of decreasing Pt(0) and increasing Pt(IV) contents was observed over formic acid-pretreated Pt/TiO_2 after repetitive mineralisation of phenol, BQ and HQ (Fig. 8). Almost no change in Pt(0) content and a smaller increase in Pt(IV) content was measured after photocatalytic mineralisation of THB (Fig. 8). This agrees well with the absence of a reductive path after the short-circuit equilibrium. Although not discussed in details here, we have observed a more drastic decrease in Pt(0) and increase in Pt(IV) contents using similar concentration of sucrose (Fig. 6), a compound which was earlier proposed to undergo a reductive pathway [15,34,36]. The observation reiterates the significance of organic degradation pathway in dictating the fate of Pt oxidation states.

4. Conclusions

An intimate relationship between the Pt oxidation state dynamics and the photocatalytic degradation mechanism of various model organic compounds was presented in this work. During the repetitive photocatalytic mineralisation of formic acid by FSP-made 0.5 at% Pt/TiO_2 consisting of predominantly Pt(II), formation of highly reductive formate free radicals resulted in the partial reduction of Pt(II) to Pt(0). As for the photocatalytic mineralisation of methanol, no formation of Pt(0) could be observed inferring the absence of current doubling effect under the studied condition. Instead, Pt(IV) was formed at the expense of Pt(II) under the experimental air-equilibrated conditions possibly due to lack of methanol (electron donor) on the photocatalyst surface. Pretreatment with formic acid increased the subsequent photocatalytic mineralisation rates of methanol, thereby demonstrating the beneficial effect of Pt(0) which was partially attributed to the dark catalytic interaction.

The photocatalytic mineralisation rates of phenol over as-prepared and pretreated Pt/TiO_2 were found to be limited by the BQ/HQ short-circuit equilibrium. As a result of the combined oxidative–reductive pathway, an increase in both Pt(0) and Pt(IV) contents was detected. Similar photocatalytic mineralisation rates of phenol, BQ and HQ were measured over as-prepared Pt/TiO_2. The co-existence of BQ/HQ had limited the overall enhancement effect. Mineralisation rates over THB, the immediate species after the BQ/HQ equilibrium, were significantly enhanced over as-prepared sample and even more so for the pretreated sample, affirming the rate-limiting step of BQ/HQ. The enhanced photocatalytic mineralisation rates over pretreated Pt/TiO_2 reported in this work could all be related qualitatively to the intimate dark catalytic interaction between the organic matters and Pt(0). Comparable trends of decreasing Pt(0) and increasing Pt(IV) contents could be observed in the case of repetitive mineralisation of phenol, BQ and HQ over the pretreated photocatalyst, corroborating the dominant electron shuttle effect, while less change in Pt oxidation states was observed after repeated photocatalytic mineralisation of THB.

The study signifies the fundamental importance of Pt oxidation state in the photocatalytic mineralisation of organic compounds. The interdependencies cannot be generalised but they are governed by the degradation pathway of the specific organic compound and its interaction with Pt. Although the present study is only limited to Pt/TiO_2, the intricate inter-relationship between deposit oxidation states and the photocatalytic mineralisation mechanism of organic compounds should be applicable to other noble metal systems.

Acknowledgments

The authors thank Prof. S.E. Pratsinis (ETH Zürich) for helpful comments and suggestions. L.M. acknowledges the German Research Association (DFG) for support under the Forschungsstipendium MA3333/1-1. This work was produced with the financial assistance of the Australian Research Council under the ARC Centres of Excellence Program.

References

[1] S. Sato, J.M. White, Chem. Phys. Lett. 72 (1980) 83.
[2] S. Sato, J.M. White, J. Catal. 69 (1981) 128.
[3] S. Nakabayshi, A. Fujishima, K. Honda, Chem. Phys. Lett. 102 (1983) 464.

[4] T. Abe, E. Suzuki, K. Nagoshi, K. Miyashita, M. Kaneko, J. Phys. Chem. B 103 (1999) 1119.
[5] R. Abe, K. Sayama, H. Arakawa, Chem. Phys. Lett. 371 (2003) 360.
[6] D.F. Ollis, H. Al-Ekabi, Photocatalytic Purification and Treatment of Water and Air, Elsevier, Amsterdam, 1993.
[7] M. Anpo, M. Takeuchi, J. Catal. 216 (2003) 505.
[8] A.V. Vorontsov, V.P. Dubovitskaya, J. Catal. 221 (2004) 102.
[9] F. Denny, J. Scott, K. Chiang, W.Y. Teoh, R. Amal, J. Mol. Catal. A Chem. 263 (2007) 93.
[10] B. Kraeutler, A.J. Bard, J. Am. Chem. Soc. 100 (1978) 4317.
[11] B. Kraeutler, A.J. Bard, J. Am. Chem. Soc. 100 (1978) 5985.
[12] W.W. Dunn, Y. Aikawa, A.J. Bard, J. Am. Chem. Soc. 103 (1981) 6893.
[13] B. Pal, S. Ikeda, H. Kominami, Y. Kera, B. Ohtani, J. Catal. 217 (2003) 152.
[14] A. Dobosz, A. Sobczyński, Water Res. 37 (2003) 1489.
[15] V. Vamathevan, R. Amal, D. Beydoun, G. Low, S. McEvoy, Chem. Eng. J. 98 (1–2) (2004) 127.
[16] H. Tran, K. Chiang, J. Scott, R. Amal, Photochem. Photobiol. Sci. 4 (2005) 565.
[17] C.-M. Wang, A. Heller, H. Gerischer, J. Am. Chem. Soc. 114 (1992) 5230.
[18] N. Chandrasekharan, P.V. Kamat, J. Phys. Chem. B 104 (2000) 10851.
[19] V. Subramaniam, E.E. Wolf, P.V. Kamat, J. Am. Chem. Soc. 126 (2004) 1943.
[20] P. Pichat, M.-N. Mozzanega, J. Disdier, J.-M. Herrmann, Nouv. J. Chim. 6 (11) (1982) 559.
[21] H. Courbon, J.-M. Herrmann, P. Pichat, J. Catal. 72 (1981) 129.
[22] H. Courbon, J.-M. Herrmann, P. Pichat, J. Phys. Chem. 88 (1984) 5210.
[23] J.-M. Herrmann, J. Disdier, P. Pichat, J. Phys. Chem. 90 (1986) 6028.
[24] N. Jaffrezic-Renault, P. Pichat, A. Foissy, R. Mercier, J. Phys. Chem. 90 (1986) 2733.
[25] J. Lee, W. Choi, J. Phys. Chem. B 109 (2005) 7399.
[26] T. Sano, N. Negishi, K. Uchino, J. Tanaka, S. Matsuzawa, K. Takeuchi, J. Photochem. Photobiol. A Chem. 160 (2003) 93.
[27] M. Koudelka, J. Sánchez, J. Augustynski, J. Phys. Chem. 86 (1982) 4277.
[28] Z. Kasarevic-Popovic, D. Behar, J. Rabani, J. Phys. Chem. B 108 (2004) 20291.
[29] M.C. Blount, J.A. Bucholz, J.F. Falconer, J. Catal. 197 (2001) 303.
[30] V. Keller, P. Bernhardt, F. Garin, J. Catal. 215 (2003) 129.
[31] K. Drew, G. Girishkumar, K. Vinodgopal, P.V. Kamat, J. Phys. Chem. B 109 (2005) 11851.
[32] W. Rachmady, M.A. Vannice, J. Catal. 192 (2000) 322.
[33] W.-R. Huck, T. Bürgi, T. Mallat, A. Baiker, J. Catal. 205 (2002) 213.
[34] W.Y. Teoh, L. Mädler, D. Beydoun, S.E. Pratsinis, R. Amal, Chem. Eng. Sci. 60 (2005) 5852.
[35] M. Abdullah, G.K.-C. Low, R.W. Matthews, J. Phys. Chem. 94 (1990) 6820.
[36] W.Y. Teoh, F. Denny, R. Amal, D. Friedmann, L. Mädler, S.E. Pratsinis, Top. Catal. 44 (2007) 489.
[37] L. Mädler, T. Sahm, A. Gurlo, J.-D. Grunwaldt, N. Barsan, U. Weimer, S.E. Pratsinis, J. Nanopart. Res. 8 (2006) 783.
[38] C. He, Y. Xiong, X. Zhu, X. Li, Appl. Catal. A Gen. 275 (2004) 55.
[39] G. Wang, Y. Lin, X. Xiao, X. Li, W. Wang, Surf. Interface Anal. 36 (2004) 1437.
[40] S.W. Lam, K. Chiang, T.M. Lim, R. Amal, G.K.-C. Low, J. Photochem. Photobiol. A Chem. 187 (2007) 127.
[41] W.H. Koppenol, J.D. Rush, J. Phys. Chem. 91 (1987) 4429.
[42] H.A. Schwarz, R.W. Dodson, J. Phys. Chem. 93 (1989) 409.
[43] S. Somansundaram, Y. Ming, C.R. Chenthamarakshan, Z.A. Schelly, K. Rajeshwar, J. Phys. Chem. B 108 (2004) 4784, and Refs. [14–20] therein.
[44] V.N. Park, N.G. Ventov, Russ. J. Phys. Chem. 49 (1975) 1489.
[45] K.-D. Asmus, H. Mockel, A. Henglein, J. Phys. Chem. 77 (1973) 1218.
[46] Y. Nosaka, H. Sasaki, K. Norimatsu, H. Miyama, Chem. Phys. Lett. 105 (1984) 456.
[47] N. Hykaway, W.M. Sears, K. Morisaki, S.R. Morrison, J. Phys. Chem. 90 (1986) 6663.
[48] R. Memming, Semiconductor Electrochemistry, Wiley–VCH, Weinheim, New York, 2001.
[49] O. Carp, C.L. Huisman, A. Reller, Prog. Solid State Chem. 32 (2004) 33.
[50] C.Y. Wang, R. Pagel, D. Bahnemann, J.K. Dohrmann, J. Phys. Chem. B 108 (2004) 14082.
[51] B. Ohtani, M. Kakimoto, S. Nishimoto, T. Kagiya, J. Photochem. Photobiol. A Chem. 70 (1993) 265.
[52] G.E. Adams, B.D. Michael, R.L. Willson, Radiation Chemistry, in: R.E. Gould (Ed.), Adv. Chem. Ser., vol. 81, American Chemical Society, Washington, DC, 1968, p. 289.
[53] L. Sun, J.R. Bolton, J. Phys. Chem. 100 (1996) 4127.
[54] T. Mallat, A. Baiker, Catal. Today 19 (1994) 247.
[55] Z. Hu, V. Boiadjiev, T. Thundat, Energy Fuels 19 (2005) 855.
[56] A. Nagasaki, H. Sakai, M. Shimazaki, T. Kakihara, T. Kono, N. Momozawa, M. Abe, Shikizai Kyokaishi 72 (11) (1999) 665.
[57] J. Theurich, M. Lindner, D.W. Bahnemann, Langmuir 12 (1996) 6368.
[58] A. Sobczyński, Ł. Duczmal, W. Zmudzinski, J. Mol. Catal. A Chem. 213 (2004) 225.
[59] B. Sun, A.V. Vorontsov, P.G. Smirniotis, Langmuir 19 (2003) 3151.
[60] C.A. Emilio, M.I. Litter, M. Kunst, M. Bouchard, C. Colbeau-Justin, Langmuir 22 (2006) 3606.
[61] A. Sobczyński, Ł. Duczmal, A. Dobosz, Monatsh. Chem. 130 (1999) 377.
[62] C. Richard, New J. Chem. 18 (1994) 443.